25th ABCM International Congress of Mechanical Engineering
October 20-25, 2019, Uberlândia, MG, Brazil

COB-2019-0302
FORCES ESTIMATION IN AUTOMOTIVE ENGINE MOUNTS BASED ON VIRTUAL SENSING TECHNIQUES

Alexandre Carlos Rodrigues Ramos
Escola de Engenharia de São Carlos, Universidade de São Paulo, Av. Trabalhador São Carlense, 13566-590, São Carlos, Brasil
alexandre.ramos@usp.br

Ricado Álvarez-Briceño
Escuela Politécnica Nacional, Av. Ladron de Guevera. P170525, Quito, Equador.
r.alvarezbriceno@gmail.com

César Abrahão Pereira Melo
Centro Federal de Educação Tecnológica de Minas Gerais, Av. Amazonas, 30510-00, Belo Horizonte, Brasil
cesarabrahao@gmail.com

Leopoldo Pisanelli Rodrigues de Oliveira
Escola de Engenharia de São Carlos, Universidade de São Paulo, Av. Trabalhador São Carlense, 13566-590, São Carlos, Brasil
leopro@sc.usp.br

Abstract. *Forces estimations are very important in the context of noise, vibrations and harshness (NVH) for certain applications as for the calculation of the frequency responses functions of a structure, modal analysis, transfer path analysis among others. A solution to identify the forces could be the direct measurement with the use of force sensors, however, in most cases, these forces cannot be measured directly or require a large investment in instrumentation and measurement capabilities. In addition, various types of force sensors can modify the dynamic characteristics of the system. More recently, probabilistic techniques based on the Kalman filter have gained importance in the field of force estimation. These techniques allow estimation of input forces in a linear system based on a limited number of measurements in a practical and efficient manner that can even deal with variability and uncertainty regarding system dynamics and input forces. In this article, an academic test-rig that simulates the excitation of an automotive engine by means of a shaker, its mounts represented by springs and structure representing the body are tested. Acceleration data and dummy measurements are obtained and the force results of the recursive probabilistic method of Kalman filters are estimated and compared with the force measured by a force sensor. The results showed a moderate relation between the forces estimated through accelerometers and dummy measurements with the results of the force sensor for certain points of application.*

Keywords: *Kalman Filter, Force Estimation, Sensor fusion, probabilistic techniques*

1. INTRODUCTION

The growing demand for quieter vehicles and with better levels of vibratory and acoustic comfort for passengers has made the Noise, Vibration and Harshness (NVH) area increase over the last decade, becoming one of the main areas related to the perception of customer quality in vehicles (Diez-ibarbia et al., 2017) and are decisive for the purchase of the product (Ramos et al., 2016). Forces estimation in mechanical systems is important, since it allows the identification of the frequencies responses functions of the system, stress and local deformation, to perform experimental modal analysis, transfer path analysis and so on.

A solution for identifying the loads could be the direct measured with the use of force sensors, however in most practical cases these forces cannot be measured directly or require a large investment in instrumentation and measurement resources (Oktav et al., 2017, Padilha et al., 2006, Seijs et al., 2015). In addition, various types of force sensors can modify the dynamic characteristics of the system, depending on their size and consequently, all the path contributions will be affected (Franklin et al., 1998). In this cases, indirect methods are required to estimate these forces. Indirect methods are especially important in cases where the force signals are unmeasurable in practice, in terms of cost and space for sensor attachments, into the measurement setup and particularly in the case of distributed forces. This paper compares the force estimated by the probabilistic method of Kalman filters (AKF-DM) using accelerometers

and dummy measurements method with the force measured by a conventional force sensor. The assay system is an academic test-rig that simulates an automotive powertrain system.

2. MECHANICAL SYSTEM MODEL AND KALMAN FILTER ALGORITHM

2.1 Mechanical model equations

Mechanical systems can be conveniently expressed in terms of modal parameters obtained via experimental procedures, such as those in Experimental Modal Analysis (EMA). In this way, the system can be represented by a system of decoupled differential equations given by equation 1.

$$\ddot{\eta} + 2\Lambda\Omega\dot{\eta} + \Omega^2\eta = \Psi^T bf + \Psi^T b_d f_d \tag{1}$$

Where η is the vector of modal coordinates, which in turn is related to the vector of physical displacement coordinates, ξ as in equation 2.

$$\xi = \Psi\eta \tag{2}$$

Where Ψ is the displacement modal matrix. Furthermore, the modal damping and natural frequencies matrices, Λ and Ω, respectively, complete the model of the system in the modal space. These matrices are defined by equation 3.

$$\Omega = \begin{bmatrix} \backslash & & \\ & \omega_r & \\ & & \backslash \end{bmatrix}, \qquad \Lambda = \begin{bmatrix} \backslash & & \\ & \xi_r & \\ & & \backslash \end{bmatrix} \tag{3}$$

Where ω_r and ζ_r are the natural frequency and damping ratio of the rth vibration mode, respectively. Moreover, the vectors f and f_d represent the external forces and unknown disturbances, which are applied on the modeled structure at physical generalized coordinates specified by the Boolean selection matrices b and b_d.
From a computational point of view, it is more convenient to represent the structure dynamics as a system of first order differential equations, which is referred to as state space model (De Oliveira et al., 2009). In this way, Eq. (1) can be written as state space model in Eq. (4) and Eq. (5).

$$\dot{x}_s(t) = Ax_s(t) + Bu(t) + B_1 w(t) \tag{4}$$

With measurement equation given by:

$$y(t) = Hx_s(t) + v(t) \tag{5}$$

Where $\dot{x_s}(t)$ is the state vector that is composed by the modal coordinates and the corresponding time derivatives $\{\eta, \dot{\eta}\}^T$, $u(t)$is the input vector, $y(t)$is the vector of measurements, and $w(t)$ and $v(t)$ are the process and measurement noise vectors, respectively.
The state matrix A, the input matrix $B$and disturbance matrix B_1 can be formulated in the modal terms defined above by the equations 6.

$$A = \begin{bmatrix} 0 & I \\ -\Omega^2 & -2\Lambda\Omega \end{bmatrix}, \qquad B = \begin{bmatrix} 0 \\ \Psi^T b \end{bmatrix}, \qquad B_1 = \begin{bmatrix} 0 \\ \Psi^T b_d \end{bmatrix} \tag{6}$$

The measurement matrix H is used to theoretically formulate the measurements as a linear combination of the states. Thus, it depends on the instrumentation used for system observation. Equations (4) and eq. (5) are presented in continuous time domain. However, the simulation analysis using the KF algorithm is performed by sampling the system dynamics at regular time intervals. Therefore, it is necessary to express the model in discrete time domain as in Eq. (7) and Eq. (8), i.e. recursive difference equations (Simon, 2006).

$$x_s(k+1) = \Phi x_s(k) + \Gamma u(k) + \Gamma_1 w(k) \tag{7}$$

With measurements

$$y(k) = Hx_s(k) + v(k) \tag{8}$$

Where Φ, Γ *and* Γ_1 are the discrete versions of previously defined matrices A, B and B_1 respectively. Continuous time versions of matrices can be transformed into their discrete time version through several methods. Actually, some of them are already implemented in MATLAB. In the present study, the zero-order hold (ZOH) method is adopted.
Regarding the characteristics of process and measurement noise, it can be assumed that they are random stationary sequences, mutually uncorrelated, with zero mean and have no time correlation that can be considered as white noises as eq. (9) and eq. (10):

$$E\{w(k)\} = E\{v(k)\} = 0 \tag{9}$$

$$E\{w(i)w^T(j)\} = E\{v(i)v^T(j)\} = 0 \qquad if \quad i \neq j \tag{10}$$

And their covariance are defined by equation 11 as detailed in (Astroza et al., 2016; Naets et al., 2015; Franklin, 1998).

$$E\{w(k)w^T(k)\} = R_w\,, \qquad E\{v(k)v^T(k)\} = R_v \tag{11}$$

2.2 Force estimation by the method of Augmented-state Kalman Filter

The Kalman filter algorithm (Naets et al.,2015; Berg and Miller, 2010) can be defined as a recursive linear state estimator, which is designed to be optimal in a minimum-variance unbiased sense (Astroza et al., 2016).
The most important idea behind this algorithm is to calculate the best estimate of x_s, $\hat{x}_s(k)$ by combining a previous estimate $\bar{x}_s(k)$ with the current measurement $\bar{y}(k)$, based on the relative accuracy of both, which is in terms of the covariance of the prior estimate, G(k), and the covariance of the measurements Rv.
The discrete form of the KF algorithm can be organized in two stages: measurement update, eq. (12) and eq. (13), and time update, eq. (14) and eq. (15) (Franklin, 1998).

$$\hat{x}_S(k) = \bar{x}_s(k) + P(k)H^T R_v^{-1}(y(k) - H\bar{x}_s(k)) \tag{12}$$

$$P(k) = G(k) + G(k)H^T(HG(k)H^T + R_v)^{-1}\,HG(k) \tag{13}$$

$$\bar{x}_s(k+1) = \Phi\hat{x}_S(k) + \Gamma u(k) \tag{14}$$

$$G(k+1) = \Phi \mathrm{P}(k)\Phi^T + \Gamma_1 R_w \Gamma_1^T \tag{15}$$

Where the initial conditions for $\bar{x}_s(0)$ and $\mathrm{G}(0)$ have to be assumed some value at algorithm initialization. The system equations can be rearranged in order to allow the coupled state - force estimation. Therefore, the input vector can be included in the state vector and predicted states via KF algorithm will estimate the forces. However, a drawback of this notation is the lack of knowledge on the dynamics relating $\dot{u}$ to the augmented state vector, now composed by$\{\eta, \dot{\eta}, u\}^T$. This lack of knowledge can be modeled conveniently as a zero-order random walk.

$$\dot{u}(t) = 0 + z(t) \tag{16}$$

Where $z(t)$ represents the unknown force variation, which is represented as a stochastic process associated to the covariance matrix R_z. In this manner, Eq. (7) can be arranged to allow augmented state vector, as detailed in Berg and Miller, 2010.

$$\begin{bmatrix} x_s(k+1) \\ u(k+1) \end{bmatrix} = \begin{bmatrix} \Phi & \Gamma \\ 0 & b \end{bmatrix}\begin{bmatrix} x_s(k) \\ u(k) \end{bmatrix} + \begin{bmatrix} \Gamma_1 & 0 \\ 0 & \Delta tb \end{bmatrix}\begin{bmatrix} w(k) \\ z(k) \end{bmatrix}, \qquad \begin{bmatrix} w(k) \\ z(k) \end{bmatrix} \sim N\left(0, \begin{bmatrix} R_w & 0 \\ 0 & R_z \end{bmatrix}\right) \tag{17}$$

Where Δt is the time step. In addition, the measurement equation for the augmented state in Eq. (17) and in case of acceleration measurements on each DOF is given by equation 18.

$$y(k) = [-\Psi\Omega^2 \;\; -2\Psi\Lambda\Omega \;\; \Psi\Psi^T b][x_s(k)\; u(k)\,] + v(k)\,, \qquad v(k) \sim N(0, R_v) \tag{18}$$

In this manner, the AKF for coupled state - force estimation and acceleration measurements can be implemented by substituting the non-starred matrices by the starred ones in equations 11 to 14 to the equations 19.

$$\Phi^* = \begin{bmatrix} \Phi & \Gamma \\ 0 & b \end{bmatrix}, \quad \Gamma^* = 0\,, \quad \Gamma_1^* = \begin{bmatrix} \Gamma_1 & 0 \\ 0 & \Delta tb \end{bmatrix}, \quad R_w^* = \begin{bmatrix} R_w & 0 \\ 0 & R_z \end{bmatrix}, \quad H^* = [-\Psi\Omega^2 \;\; -2\Psi\Lambda\Omega \;\; \Psi\Psi^T b] \tag{19}$$

3. EXPERIMENTAL ASSEMBLY

The system simulates an automotive powertrain which it has a source of excitation, pathways and targets. The excitation consists of a coupled steel frame with an inertial shaker (model 2002E) that simulates the excitation of the vehicular engine, the paths are represented by three springs (stiffness 2.697N/m) coupled to force sensors, the receiver side is called a passive-system and is represented by the aluminum plate, that simulates a vehicle body and suspension springs which assume to be an automotive suspension system (stiffness 14.400 N/m). The instrumentation consists of three force sensor (PCB models 208A12, 208C02 and Y208C01), twelve uniaxial accelerometers (PCB 333B, 352C34 and 352C22 models). The acquisition system used for the analysis and for force estimation was the LMS SCADAS Mobile, with a rectangular windowing, with 2048 Hz of bandwidth, a resolution of 0.25 Hz, totalizing 8192 spectral lines for all 16 channels.

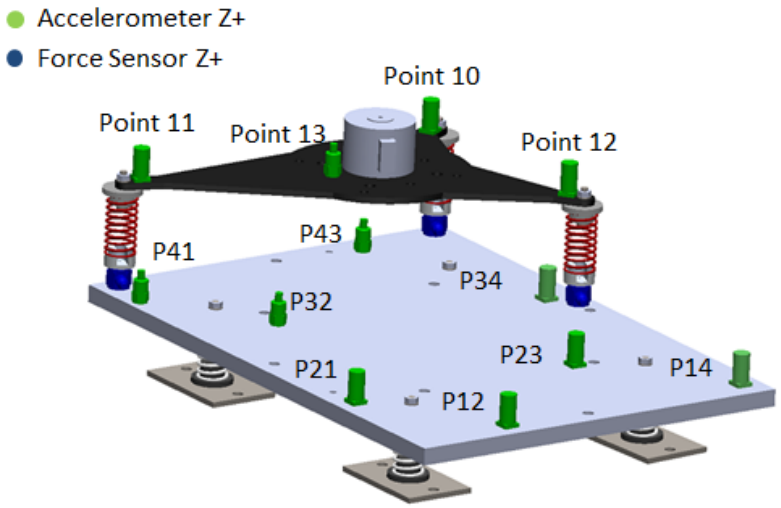

Figure 1. Academic Powertrain System

The experimental tests were performed in three stages where points 10, 11 and 12 were independently excited with an external shaker and the acceleration responses were measured, the accelerometers installed on the passive plate were used to identify the dynamics of the system under study, as shown in figure 2.

Figure 2. Powertrain system excited on point 12 by a shaker

In the Figure 3 below it is possible to observe the coherence of all sensors in the frequency range of 0 to 800 Hz, for some sensors the value is below 0.75, particularly between frequencies of 90.63 Hz and 218.93 Hz, 332.13 Hz at 411.39 Hz and 617.26 Hz at 666.45 Hz.

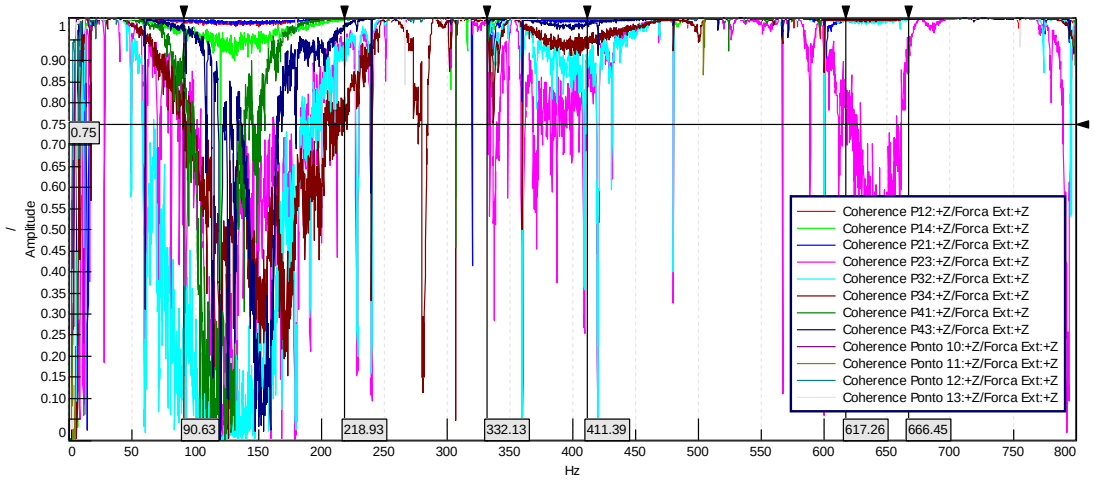

Figure 3. Coherences of all accelerometers

Thus, nine degrees of freedom were chosen to represent the powertrain system, being the DOFs represented by the points P12, P21, P34, P41, P43, point 10, point 11, point 12 and point 13 that presented smaller variances and better coherences as can be observed in figure 4. It is noted for P34, P41 and P43 sensors coherencies below 0.75, but no natural frequencies were observed in the frequency range of 32.24 Hz to 260.48 Hz as can be noted in Table 1.

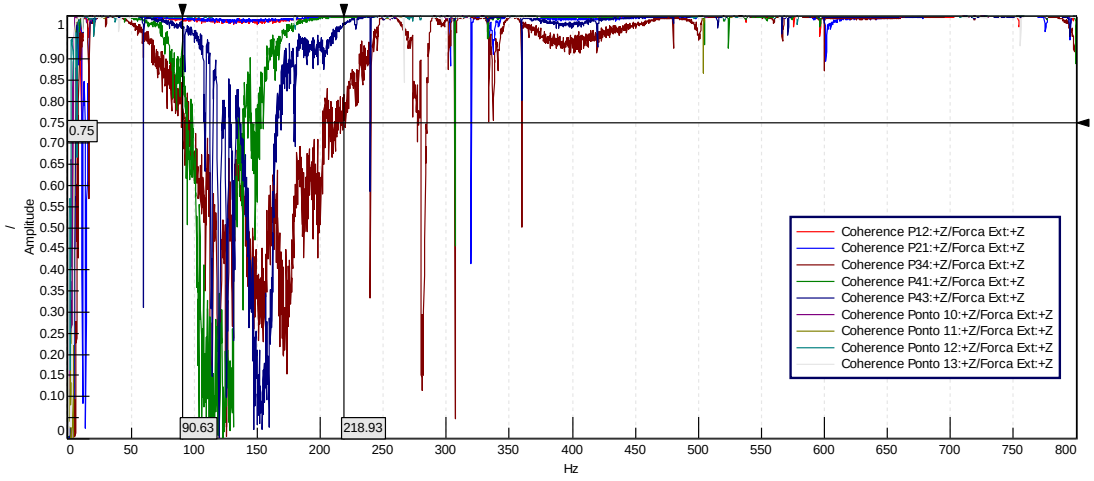

Figure 4. Coherence of the chosen accelerometers

The eigenvalues and eigenvectors of the powertrain system were selected along with their damping ratio and synthesized for Kalman filter application.

Table 1: Natural frequencies and dumping ratios of the powertrain system

f_1[Hz]	f_2[Hz]	f_3[Hz]	f_4[Hz]	f_5[Hz]	f_6[Hz]	f_7[Hz]	f_8[Hz]	f_9[Hz]
11.324	29.295	32.244	260.480	315.609	352.466	577.471	676.832	763.832
ζ_1	ζ_2	ζ_3	ζ_4	ζ_5	ζ_6	ζ_7	ζ_8	ζ_9
1.07%	2.24%	0.86%	0.11%	0.08%	0.09%	0.05%	0.14%	0.33%

4. RESULTS

The curves of the three excited points, point 10, point 11 and point 12, were plotted in the time domain and in the frequency domain by power spectrum density (PSD). In figure 5 it can be seen that the predicted data showed a deviation of the force applied with a gain compared to that measured by the force sensor at the point 10 and when the energy level is analyzed, figure 6, in the range of 0 to 30 Hz and above of 500 Hz it has an estimated curve behavior close of the measured curve with a slightly higher amplitude.

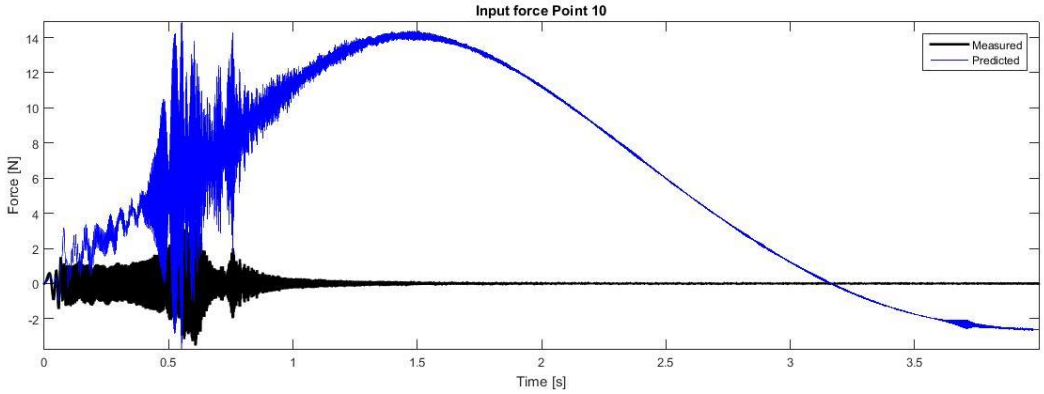

Figure 5. Time-domain response of point 10

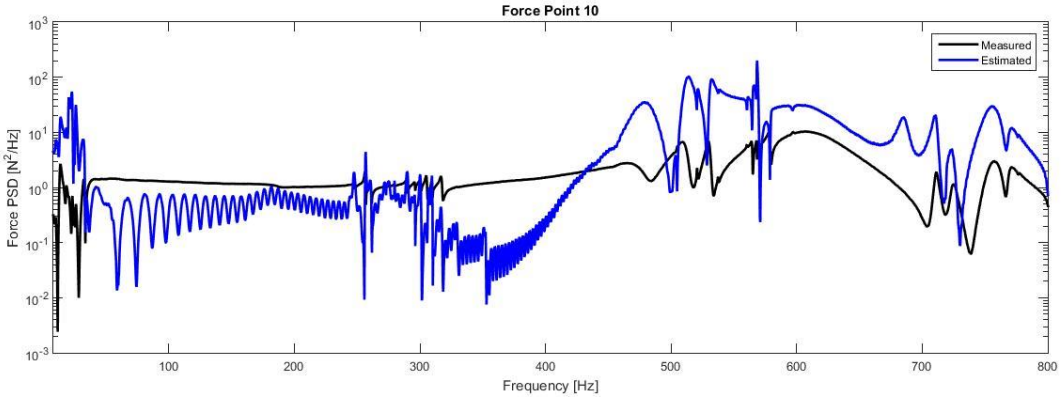

Figure 6. Power Spectrum Density of Point 10

In Figure 7 it can be seen that the data provided on point 11 showed a deviation of the applied force with a gain compared to that measured by the force sensor. When the power level is analyzed, figure 8, in the range of 0 to 30 Hz, 210 to 320 Hz and above 500 Hz it has an estimated curve behavior close, with a higher level of energy, to that of the measured curve.

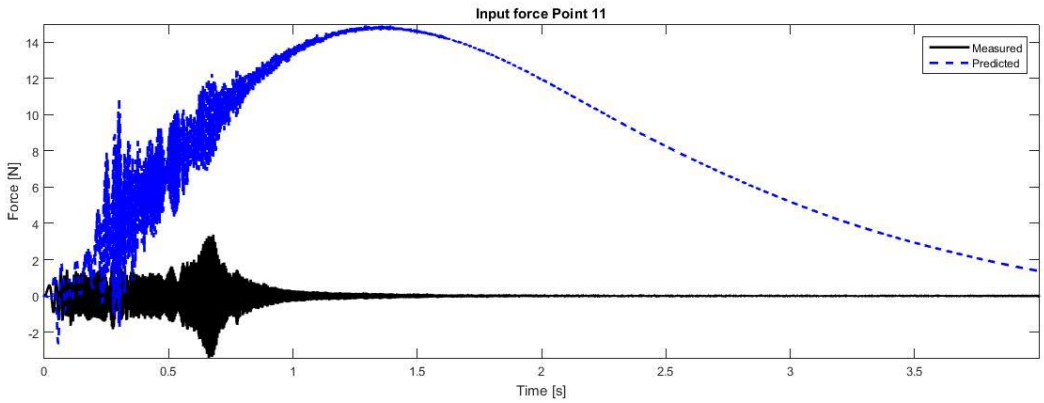

Figure 7. Time-domain response of point 11

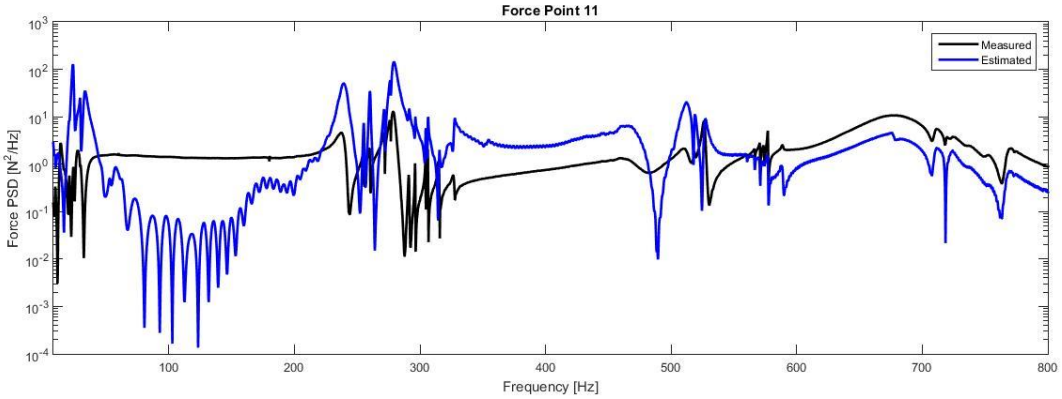

Figure 8. Power Spectrum Density of Point 11

In figure 9 it can be seen that the data predicted on point 12 showed a deviation of the force applied with a gain compared to that measured by the force sensor in the location and when the power level, figure 10, is analyzed in the range of 0 to 30 Hz, 210 to 320 Hz and above 500 Hz it has an estimated curve behavior close of the measured curve with a higher level of energy.

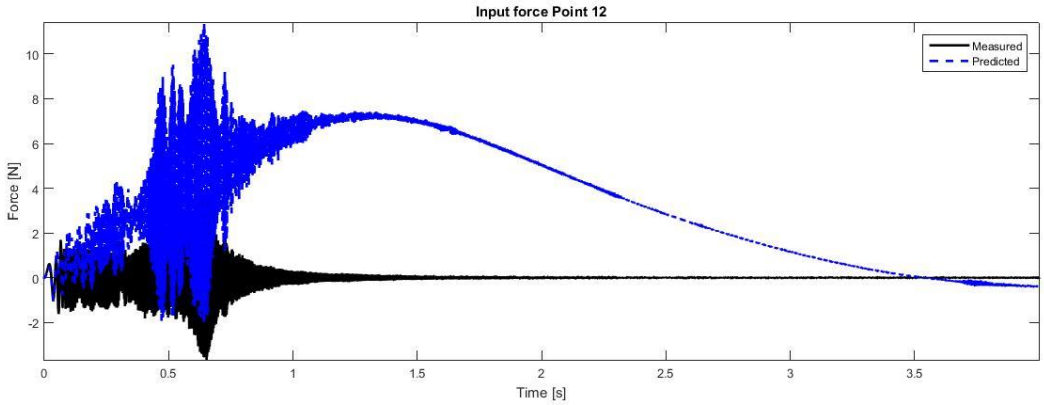

Figure 9. Time-domain response of point 12

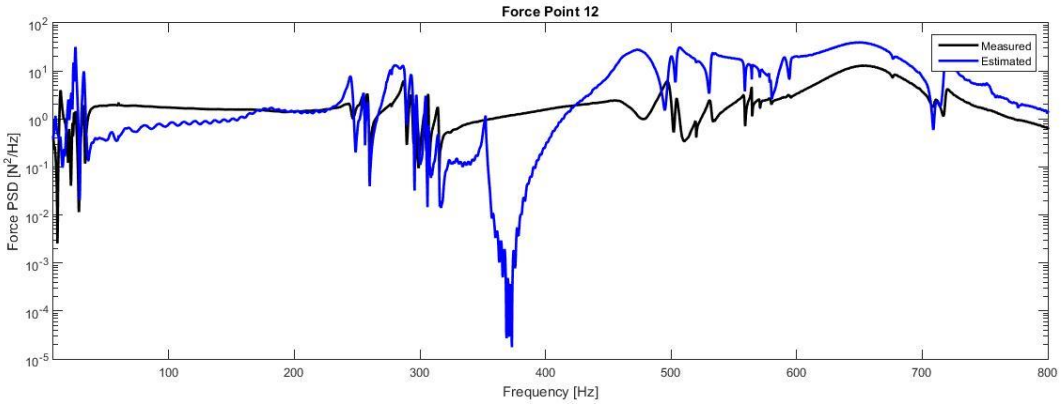

Figure 10. Power Spectrum Density of Point 12

5. CONCLUSIONS

The first natural frequency of the system is at 11 Hz. In this way, the excitation was performed by means of an external shaker due to the limitation of the inertial shaker in frequencies below 20 Hz. The stability of the kalman filter algorithm is dependent on the quality of measurements, model size, sensor positioning and accelerometer variances, nine accelerometers were selected, representing nine degrees of freedom of the powertrain system under study. The method of choice was the sensors that presented lower levels of background noise, better coherences of the measured signals and that presented all the natural frequencies of the system.

The deviations found between the measured force and the estimated force can be explained due to the assumption that the covariance matrix of the state vector is diagonal and assumed that the covariances were linearly independent when in practice they are linearly dependent and are correlated with each other being the covariance matrix non-diagonal.

It is possible to conclude from this work that the application of AKF with dummy measurements assuming a 1-D system, in the case of linearly independent accelerometers, was not totally satisfactory for force estimates, despite a certain correlation between the data obtained in the time and frequency domain. Thus, it is necessary to study other forces estimation techniques for 2-D and 3-D systems for the correct estimation of forces in complex systems.

6. ACKNOWLEDGEMENTS

The authors acknowledge the financial assistance of the Brazilian National Council for Scientific and Technological Development - CNPq (grant numbers 481044/2010-8 and 307369/2013-7) and the FP7 project EMVeM.

7. REFERENCES

Diez-ibarbia, A., Battarra, M., Palenzuela, J., Cervantes, G., Walsh, S., De-la-cruz, M., Theodossiades, S., 2017. “Comparison between transfer path analysis methods on an electric vehicle”, Applied Acoustics, 118, pp. 83–101.

Ramos, A.C.R., Santos, R.B., Melo, C.A.P., Perez, I.C.S., 2016. “Vibroacoustic transfer function study in the design of vehicle suspensions”, *SAE Technical Papers Series*, São Paulo, Brazil, pp. 7.

Oktav, G.A., Yılmaz, Ç., 2017. “Transfer path analysis: Current practice, trade-offs and consideration of damping”, *Mechanical Systems and Signal Processing*. 85, pp. 760–772.

Padilha, P.E.F., Arruda, J.R.F., 2006.“Comparison of estimation techniques for vibro-acoustic transfer path analysis”, *Shock and Vibration*, 13, pp. 459–467.

Seijs, M.V.D., Klerk, D. D., Rixen, D.J., 2015. “General framework for transfer path analysis : History, theory and classification of techniques”, *Mechanical Systems and Signal Processing* , pp. 1–28.

De Oliveira, L.P.R.,Varoto, P.S., Sas, P., Desmet, W., 2009. “A state-space modeling approach for active structural acoustic control”, *Shock and Vibration*, 16, pp. 607–621.

Franklin, G.F., Powell, J.D., Workman, M.L., 1998.“*Digital control of dynamic systems*”, Addison-Wesley.

Astroza, R., Nguyen, L.T., Nestorović, T., 2016. “Finite element model updating using simulated annealing hybridized with unscented Kalman filter”, *Computers and Structures*, 177, pp. 176–191.

Naets, F., Cuadrado, J., Desmet, W., 2015. “Stable force identification in structural dynamics using Kalman filtering and dummy-measurements”, *Mechanical Systems and Signal Processing*. 50–51, pp. 235–248.

Berg, J.C., Miller, A.K., 2010. “Force Estimation via Kalman Filtering for Wind Turbine Blade Control”, *Proceedings of the IMAC-XXVII*, Jacksonville, Florida, USA.

Hansen, P.C., 1992. “Analysis of discrete ill-posed problems by means of the L-Curve”, *Society for Industrial and Applied Mathematics*, 34, pp. 561–580.

Cumbo, R., Tamarozzi, T., Janssens, K., Desmet, W., 2019. “Kalman-based load identification and full-field estimation analysis on industrial test case”, Mechanical Systems and Signal Processing, 117, pp. 771–785.

Simon, D., 2006. "*Optimal state estimation: Kalman, H infinity, and nonlinear approaches.*", John Wiley & Sons.

Hautus, M.L.J., 1970. “Stabilization controllability and observability of linear autonomous systems”, *Proceedings of Indagationes Mathematicae*, Eindhoven, Netherlands.

Chatzi, E. N., Fuggini, C., 2012. “Structural identification of a super-tall tower by GPS and accelerometer data fusion using a multi-rate Kalman filter*”, Proceedings of the Third International Symposium on Life-Cycle Civil Engineering* , Vienna, Austria.

8. RESPONSIBILITY NOTICE

The author(s) is (are) the only responsible for the printed material included in this paper.